Environmental Science: Atmospheres

ROYAL SOCIETY OF CHEMISTRY

PAPER

View Article Online
View Journal | View Issue

Cite this: *Environ. Sci.: Atmos.*, 2022, **2**, 352

The contribution of new particle formation and subsequent growth to haze formation

Markku Kulmala, *[abc] Runlong Cai,[b] Dominik Stolzenburg,[b] Ying Zhou,[a] Lubna Dada, [bd] Yishuo Guo,[a] Chao Yan,[ab] Tuukka Petäjä, [bc] Jingkun Jiang [e] and Veli-Matti Kerminen[bc]

We investigated the contribution of atmospheric new particle formation (NPF) and subsequent growth of the newly formed particles, characterized by high concentrations of fine particulate matter ($PM_{2.5}$). In addition to having adverse effects on visibility and human health, these haze particles may act as cloud condensation nuclei, having potentially large influences on clouds and precipitation. Using atmospheric observations performed in 2019 in Beijing, a polluted megacity in China, we showed that the variability of growth rates (GR) of particles originating from NPF depend only weakly on low-volatile vapor – highly oxidated organic molecules (HOMs) and sulphuric acid – concentrations and have no apparent connection with the strength of NPF or the level of background pollution. We then constrained aerosol dynamic model simulations with these observations. We showed that under conditions typical for the Beijing atmosphere, NPF is capable of contributing with more than 100 μg m^{-3} to the $PM_{2.5}$ mass concentration and simultaneously >10^3 cm^{-3} to the haze particle (diameter > 100 nm) number concentration. Our simulations reveal that the $PM_{2.5}$ mass concentration originating from NPF, strength of NPF, particle growth rate and pre-existing background particle population are all connected with each other. Concerning the PM pollution control, our results indicate that reducing primary particle emissions might not result in an effective enough decrease in total $PM_{2.5}$ mass concentrations until a reduction in emissions of precursor compounds for NPF and subsequent particle growth is imposed.

Received 22nd November 2021
Accepted 21st March 2022

DOI: 10.1039/d1ea00096a

rsc.li/esatmospheres

Environmental significance

Air pollution is important for human health and environment. Particulate matter is one of the key elements for air pollution. We hypothesize that there are essentially three different pollution regimes for PM, corresponding to different balances between emissions and air pollution control, and having different processes dictating the PM concentration levels: (1) high primary PM emissions, resulting in high primary PM concentrations (primary dominating regime), (2) decreased primary PM emissions, yet relatively high PM precursor emissions, causing enhanced secondary PM production and partial replacement of primary PM with secondary PM (secondary dominating regime), and (3) decreased precursor emissions, resulting in an improved air quality (clean regime). Most of our simulations concern the air pollution regime 2 outlined above, in addition to which our results will shed light on the factors dictating the border between the air pollution regimes 1 and 2. Actually without understanding secondary (airborne) air pollution it is difficult to mitigate air pollution.

1 Introduction

Despite the strict air pollution control measures imposed in China during the recent years, fine particulate matter ($PM_{2.5}$) continues to have very high concentration levels, causing serious adverse health effects over most of the country.[1–4] Of special interest in this respect is the formation and persistence of haze, characterized by $PM_{2.5}$ concentrations, typically larger than a few tens of μg m^{-3}. Previous studies have demonstrated that the formation of haze in Chinese megacities is associated with a complex interplay between emissions, transportation, meteorological conditions and atmospheric chemistry.[5–14] In Beijing, atmospheric new particle formation (NPF) tends to precede the formation of haze in winter.[5,15] The contribution of NPF and subsequent gas-to-particle conversion (GTP) associated with these newly formed particles to the increased $PM_{2.5}$ mass concentrations during the haze formation has, however, remained difficult to quantify. This is partially due to challenges in separating between particles emitted by primary sources and those originating from atmospheric NPF in urban

[a]*Aerosol and Haze Laboratory, Beijing Advanced Innovation Center for Soft Matter Sciences and Engineering, Beijing University of Chemical Technology (BUCT), Beijing, China*

[b]*Institute for Atmospheric and Earth System Research (INAR)/Physics, Faculty of Science, University of Helsinki, Finland. E-mail: markku.kulmala@helsinki.fi*

[c]*Joint International Research Laboratory of Atmospheric and Earth System Sciences, School of Atmospheric Sciences, Nanjing University, Nanjing, China*

[d]*Laboratory of Atmospheric Chemistry, Paul Scherrer Institute, Villigen, Switzerland*

[e]*State Key Joint Laboratory of Environment Simulation and Pollution Control, School of Environment, Tsinghua University, Beijing, China*

environments,[16–18] and partially due to our incomplete understanding on the dynamics of clusters and aerosol particles smaller than a few nm in diameter under highly polluted conditions.[19]

In this manuscript, we investigate the contribution of NPF and subsequent GTP to both $PM_{2.5}$ mass concentration and haze particle (diameter > 100 nm) number concentration using model simulations constrained with atmospheric observations in Beijing. Our primary goal is to quantify how sensitive the $PM_{2.5}$ mass concentration increase is to the characteristics of NPF, subsequent particle growth of freshly formed particles and pre-existing background particle population. Our secondary goal is to put these results into the context of the ongoing and future air pollution control mitigation strategies. For the latter, we hypothesize that there are essentially three different pollution regimes for PM, corresponding to different balances between emissions and air pollution control, and having different processes dictating the PM concentration levels: (1) high primary PM emissions, resulting in high primary PM concentrations (primary dominating regime), (2) decreased primary PM emissions, yet relatively high PM precursor emissions, causing enhanced secondary PM production and partial replacement of primary PM with secondary PM (secondary dominating regime), and (3) decreased PM precursor emissions, resulting in an improved air quality (clean regime). Most of our simulations concern the air pollution regime 2 outlined above, in addition to which our results will shed light on the factors dictating the border between the air pollution regimes 1 and 2.

2 Methods

Particle number size distributions are continuously measured at the Aerosol and Haze Laboratory (AHL) at the west campus of the Beijing University of Chemical Technology (BUCT) from January 2018 onwards. The BUCT-AHL station is surrounded by residential and commercial areas, as well as, three main roads with a heavy traffic load. Therefore, this station can be regarded as a typical urban site. More details on the station can be found elsewhere.[20] Such long-term comprehensive observations enable us to investigate several atmospheric processes and their feedbacks. Here we use the full-year data set of 2019 as representative for the typical conditions in Beijing.

2.1. Instrumentation

Particle number size distributions were measured using a DEG-SMPS combined with conventional SMPS systems to cover the size-range of 1.5–1000 nm. The DEG-SMPS was equipped with a specially designed DMA for classifying sub 10 nm particles and a core sampling inlet for improving their sampling efficiency.[22–24] The ion number size distribution of both naturally charged positive and ions for the size-range of 0.8–42 nm was measured using a Neutral cluster and Air Ion Spectrometer (NAIS).[21] The concentration of condensable vapors, *i.e.*, sulfuric acid and oxygenated organic molecules (OOMs) are measured using a nitrate-base CI-API-ToF. The configuration of these instruments were described in detail in our previous studies.[25,26]

2.2. Data analysis

Particle growth rates (GR) in size bins 3–7 nm and 7–15 nm were calculated with several techniques. We used the 50% appearance time method[27,28] to get an estimate on $GR_{3-7\ nm}$ and $GR_{7-15\ nm}$ using our SMPS data. We further used the maximum concentration method[29] on the same dataset and the ion spectrometer data with the appearance time method to validate the first result. We rejected all GR estimates where the derivation was larger than a factor of 2 between the appearance time result from the SMPS and any of the other approaches. That way, we are highly confident that our reduced 50% appearance time GR dataset from the SMPS represents the typical variation at the AHL/BUCT station independent of the used calculation method.

2.3. Model description

The contributions of NPF to particle mass concentration are illustrated using a box model that tracks single-particle growth in the Lagrangian specification. Integrating the new particle formation rate with respect to time, we obtain the total number concentration of new particles formed during an NPF event. These new particles grow larger in size while being simultaneously scavenged by coagulation, represented using the coagulation sink (CoagS) of two particle populations: a constant background particle population and particles originating from NPF. The CoagS for particles at different sizes is calculated from the condensation sink (CS) for sulfuric acid using the Kerminen–Kulmala equation.[30] The dependency of CoagS on the new particle size, dln CoagS/dln d_p, is assumed to be –1.7 in line with our earlier observations.[30] The same investigation[30] showed that particle scavenging rates are only weakly dependent on the exact value of this parameter. We also take into account the sink due to self-coagulation, which predominates the CoagS at high cluster concentration during high particle formation rates.[32] Due to the dependency of self-coagulation on the GR, the survival probabilities (P) of new particles are solved numerically. Considering the large uncertainties in the survival probabilities of sub-3 nm particles in polluted megacities,[19] the initial size of new particles in the box model is typically taken to be 5 nm. However, we tested multiple initial sizes using our simulations to see how sensitive our simulations are to the initial size. The number concentration of growing-mode particles is calculated using eqn (1).

$$N(d_p) = P(5\ \text{nm} \rightarrow d_p) \times \int_{t1}^{t2} J_5(t)\mathrm{d}t. \quad (1)$$

The mass of the growing-mode particles and their contributions to CoagS are then calculated using $N(d_p)$, and the particle density, ρ, is assumed to be 1400 kg m^{-3}. To account for the fact that the growing-mode particles do not have exactly the same size, we assume the growing mode follows a log-normal

distribution and use the Hatch–Choate equation[33] to calculate the geometric mean diameters for mass and CoagS,

$$d_{\mathrm{mean}} = d_{\mathrm{p}} \times \exp\left\{(m + 0.5) \times \left[\ln(\sigma_{\mathrm{geo}})\right]^2\right\}, \quad (2)$$

where d_{mean} is the mode mean diameter and σ_{geo} is the geometric standard deviation of the growing mode. We assume $\sigma_{\mathrm{geo}} = 1.7$ for this study. The value of m is 3 for mass and it is a certain value as a function of d_{p} ranging between 1 and 2 for CoagS.

3 Results and discussion

Due to the crucial role of the particle growth rate in both survival of the newly formed particles and their eventual contribution to total particle mass concentrations, we started our analysis by constraining this quantity using measurements conducted in Beijing. Fig. 1 demonstrates a relatively limited variability of particle growth rates in the size ranges of 3–7 nm and 7–15 nm between the different NPF events. Even more importantly, it shows practically no dependence of the GR on either the strength of NPF (as indicated by the total particle number concentration in this size range) or the level of background pollution as measured by condensation sink, CS.

Excluding cases of extremely high initial particle number concentrations or environments with long particle residence times, both favoring particle self-coagulation,[32,34–36] the value of GR is dictated by gas-to-particle conversion (GTP). Potential GTP mechanisms in this respect are the condensation of low-volatile vapors onto the growing particles, or either thermodynamic partitioning or various multiphase reactions involving semi-volatile or volatile vapors in these particles (*e.g.* Wang *et al.*, 2010;[37] Riipinen *et al.*, 2012;[38] Riva *et al.*, 2021 (ref. 39)). Fig. 2 shows the GR in the size ranges of 3–7 nm and 7–15 nm as a function of the low-volatile vapor concentration, here highly oxidated organic molecules (HOMs) and sulphuric acid. Although there is some tendency of the GR to increase with an increasing low-volatile vapor concentration, the slope of this relation is far below unity, indicating that HOMs and sulphuric acid together cannot explain the growth, and that more volatile vapors or multiphase chemistry play important roles in the particle growth. This view is supported by the clear increase of GR with an increasing particle size (from 3–7 nm to 7–15 nm), a typical feature based on earlier findings from Beijing and other polluted environments in China.[40–45] Overall, Fig. 1 and 2 demonstrate that the variability of the GR following NPF is relatively limited compared to the most important quantities believed to influence this quantity.

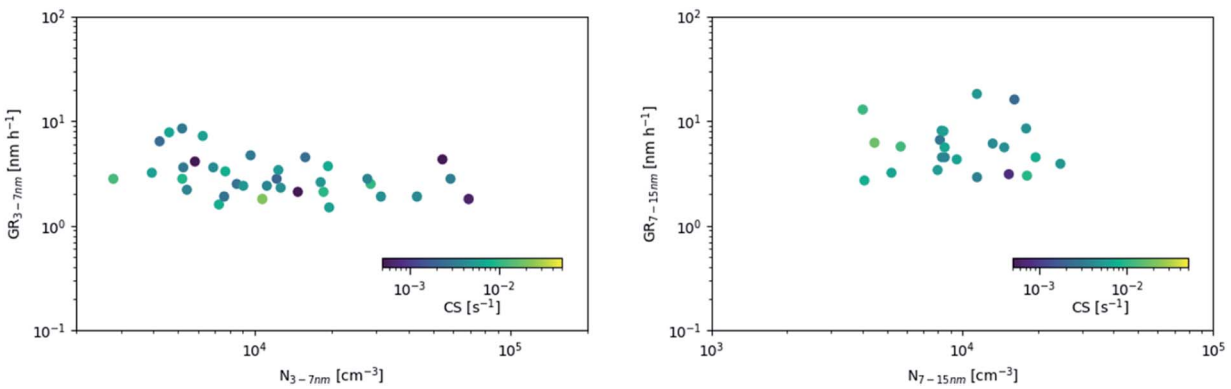

Fig. 1 Growth rates (50% appearance time measured by SMPS) of 3–7 nm (left panel) 7–15 nm (right panel) particles as a function of the total particle number concentration in the corresponding size ranges.

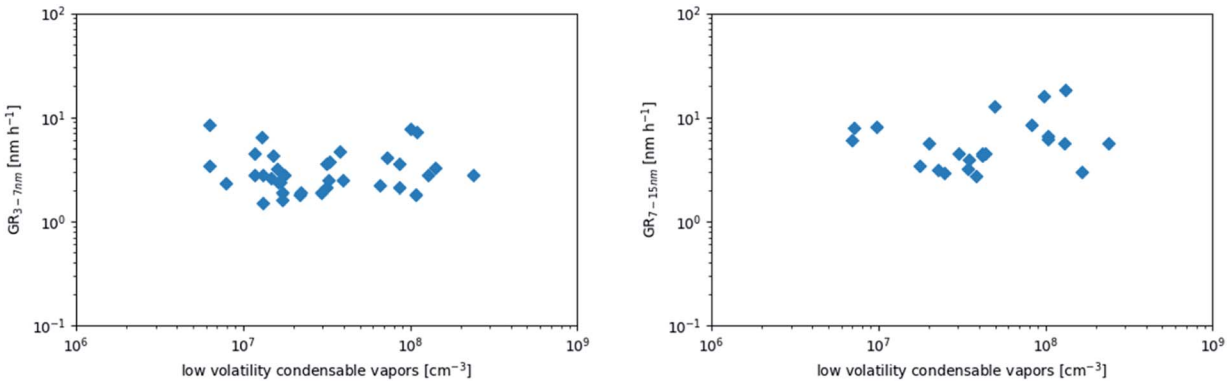

Fig. 2 Growth rates (50% appearance time measured by SMPS) of 3–7 nm (left panel) and 7–15 nm (right panel) particles as a function of the measured low-volatile vapour concentration (HOMs + sulphuric acid). Measurements are from Beijing 2019.

Next, we performed a suite of model simulations to find out how much NPF and associated GTP contributes to the $PM_{2.5}$ mass concentration, and to quantify how sensitive is this contribution to the characteristics of NPF, subsequent particle growth and pre-existing background particle population. We first illustrate how the mode of growing particles following cluster formation at 1.5 nm evolves in time when considering a typical NPF event observed at our AHL/BUCT measurement site in Beijing (Fig. 3). We see a rapid decrease in the particle number concentration and a modest increase in the mass concentration of the growing mode, approaching 10 μg m^{-3} after 48 h of simulations. This kind of behavior is mainly due to the unrealistically low survival probability of newly formed clusters during their initial growth up to a few nm, a yet unexplained feature identified already by Kulmala *et al.*[19] Therefore, we decided to start our simulations from sizes at which dynamics of the growing particle mode is more reliably constrained from atmospheric observations. We selected this size as 5 nm in most of our later simulations.

Fig. 4 is similar to the right panel of Fig. 3, but with the simulated particle growth starting from 5 nm instead of 1.5 nm. The total particle number concentration in the growing mode decreases with time due to scavenging by coagulation, approaching 1000 particles cm^{-3} after 48 hours of the simulation time. The mass of the growing mode reaches 1 μg m^{-3} within the first 6 hours, 10 μg m^{-3} in less than 20 hours, and 100 μg m^{-3} in less than 40 hours. This indicates that when there are no major synoptic-scale changes in air masses, secondary aerosol formation associated with particles originating from a typical NPF event can provide a large contribution to the $PM_{2.5}$ mass concentration, and thereby to haze.

Fig. 5 illustrates the connection between the particle formation rate at 5 nm and the mass concentration of the growing mode, M, after 48 hours of the simulation time under both polluted (left panel) and relatively clean conditions (right panel). We can see that M increases almost linearly with an increasing particle formation rate for J_5 smaller than about 1 cm^{-3} s^{-1} (left panel) and 10 cm^{-3} s^{-1} (right panel). With further increases in J_5, the increase of M first weakens and then fully saturates. The primary reason for this behavior is revealed by Fig. 6a: an increasing CS enhances the coagulation scavenging of particle in the growing mode, eventual suppressing the formation of additional particulate mass in this mode. Since both background particle population and growing mode contribute to CS, the level of M reached and its potential saturation are influenced by the pre-existing particle population and by the strength of NPF and subsequent particle growth.

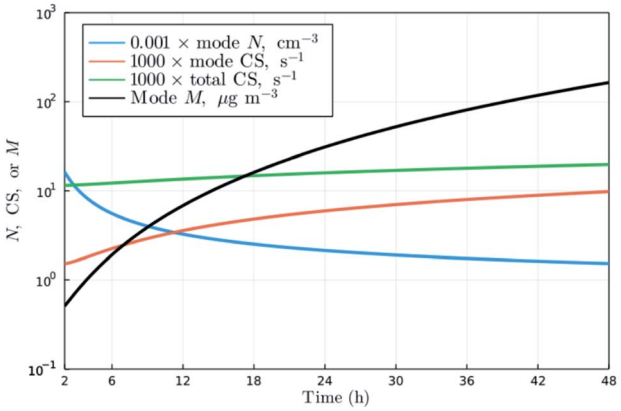

Fig. 4 Number, surface area and mass concentrations of the growing mode as function of time. The model inputs are: J_5 = 10 cm^{-3} s^{-1}, initial diameter = 5 nm, duration of NPF = 5 h, GR = 4 nm h^{-1}, $CS_{background}$ = 0.010 s^{-1} and σ_{geo} = 1.7.

The selected value of the initial diameter of the growing particle mode has a relatively small influence on the simulated mass of the growing mode, as long as this diameter does not drop much below 5 nm (Fig. 6b). The GR of the growing particle mode is substantially more influential in this respect (Fig. 6c). This is because the survival probabilities of growing particles decrease exponentially with a decreasing value of their GR,[31,46] decreasing the number of particles that will eventually accumulate mass during their growth to larger sizes.

Fig. 7 summarizes our results by showing the combined effects of the background particle population ($CS_{background}$), strength of NPF (J_5) and GR on the mass, M, by which the

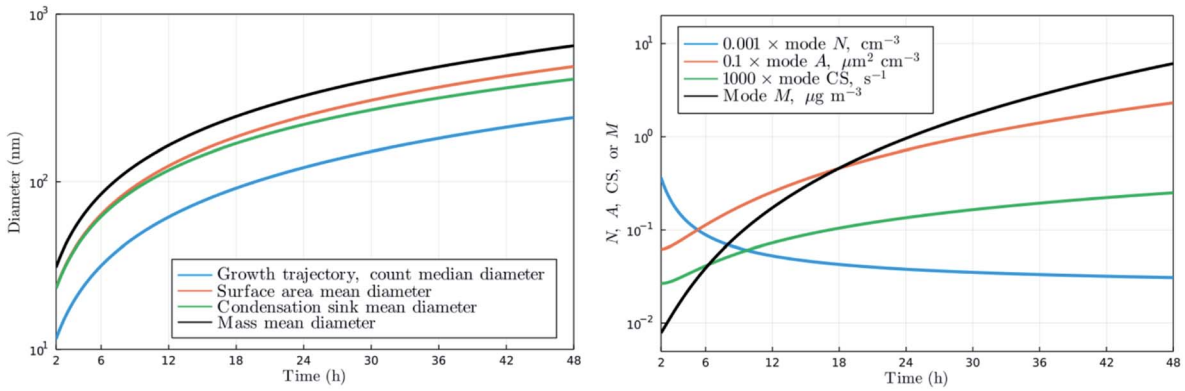

Fig. 3 Simulated growth of newly formed particles. The left panel shows different diameters of the growing mode during the model experiment, and the right panel shows the corresponding number (N), surface area (A), and mass (M) concentrations. The model inputs are: $J_{1.5}$ = 200 cm^{-3} s^{-1}, duration of NPF = 5 h, GR = 5 nm h^{-1}, CS = 0.015 s^{-1} and CS/GR = 10.8 nm^{-1}, which all are within the values observed in Beijing.[15]

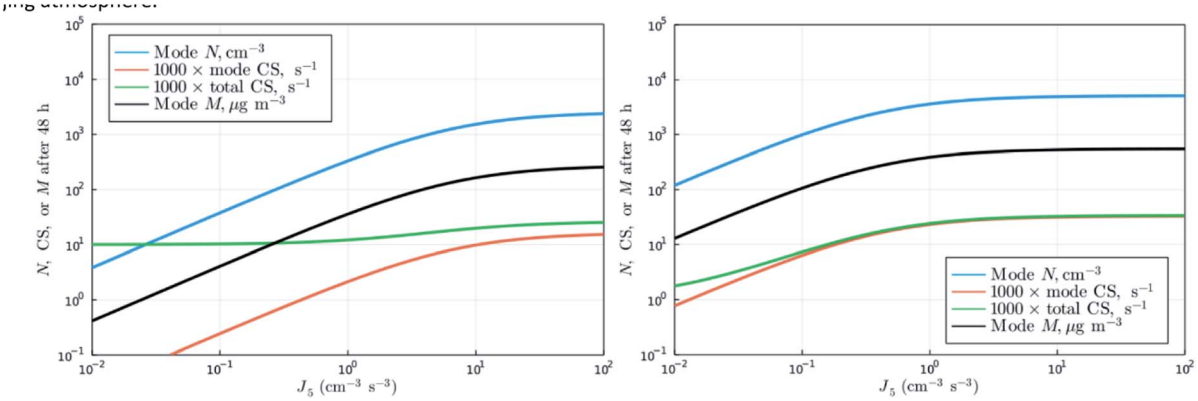

Fig. 5 Number, surface area and mass concentration of the growing mode after 48 h as function of the formation rate of 5 nm particles, J_5. The condensation sink of the background particle population, $CS_{background}$, has been assumed to be equal to 0.010 s^{-1} (left panel) or 0.001 s^{-1} (right panel). The other model inputs are: initial particle diameter = 5 nm, duration of NPF = 5 h, GR = 4 nm h^{-1} and σ_{geo} = 1.7.

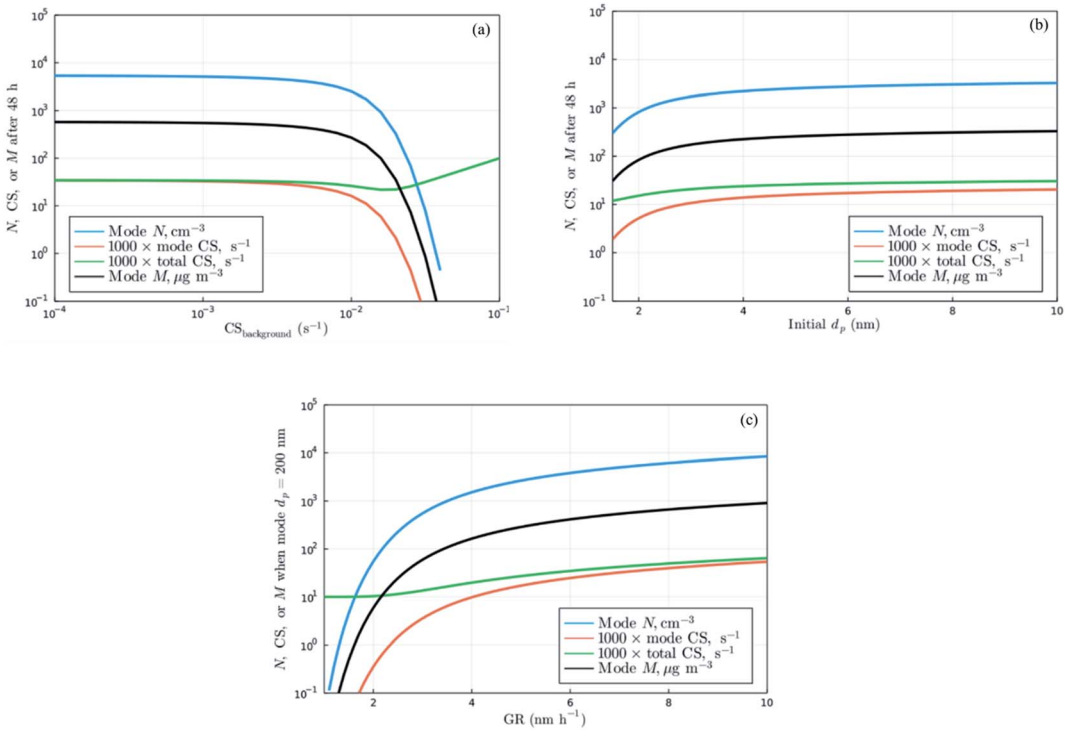

Fig. 6 Number, surface area and mass concentrations of the growing mode after 48 h as function of (a) $CS_{background}$, (b) the initial diameter of the growing mode, and (c) the growth rate, GR. Most of the particles survive with high GR and are scavenged with low GR. Note: the ending diameter is the same (200 nm) for different GRs, while the ending time varies (48 h when GR = 4 nm h^{-1}). The other model inputs are: J_5 = 10 cm^{-3} s^{-1}, duration of NPF = 5 h and σ_{geo} = 1.7; GR = 4 nm h^{-1} in (a) and (b), initial diameter of the growing mode = 5 nm in (a) and (c), and $CS_{background}$ = 0.010 s^{-1} in (b) and (c).

growing particle mode contributes to $PM_{2.5}$ after 48 h since the start of NPF. We can see that practically no new mass is produced *via* NPF and subsequent particle growth when the level of background pollution is very high ($CS_{background}$ > 0.01–0.04 s^{-1}), regardless of the values of J_5 or GR. The value of M remains moderate (<10 μg m^{-3}) when both $CS_{background}$ is large and J_5 is small, whereas even very high values of M (>100 μg m^{-3}) are possible for realistic combinations of $CS_{background}$, J_5 and GR. For example, under originally relatively clean conditions ($CS_{background}$ = 0.001 s^{-1}), M reaches >100 μg m^{-3} at J_5 = 0.1 s^{-1} when GR = 4 nm h^{-1} and at J_5 = 0.01 s^{-1} when GR = 8 nm h^{-1}. These values of J_5 are much lower than the typical formation rates of >3 nm particles reported for Beijing during NPF.[45,47–49] Under originally polluted conditions ($CS_{background}$ = 0.01 s^{-1}), the values of J_5 needed for producing M of 100 μg m^{-3} are 4.0 s^{-1} and 0.05 s^{-1} for GR = 4 and 8 nm h^{-1}, respectively. Such formation rates of up to a few particles s^{-1} can be

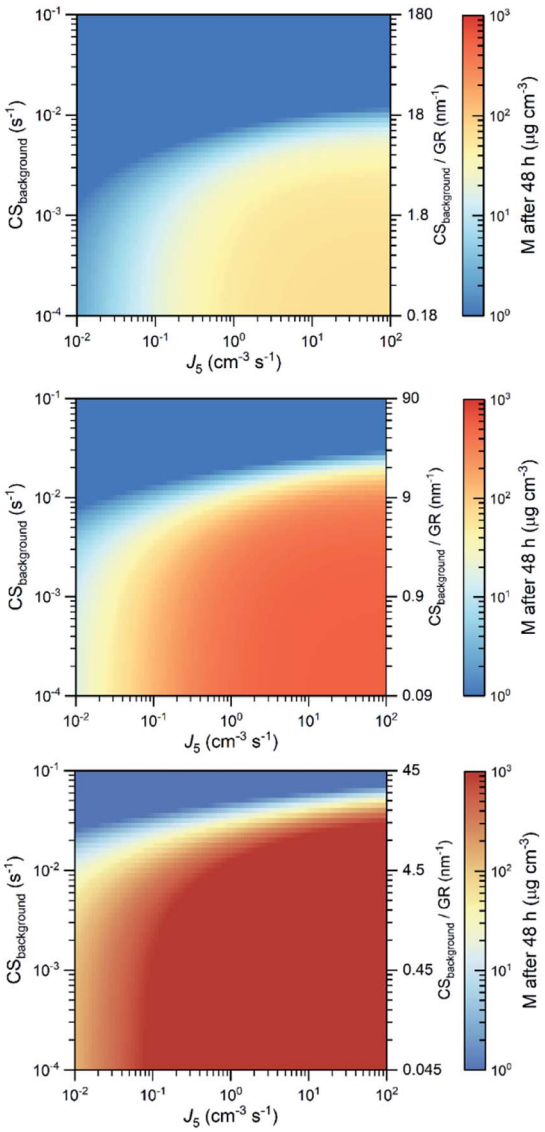

Fig. 7 Mass of the growing mode after 48 h as function of J_5 and $CS_{background}$. The other model inputs are: initial $d_p = 5$ nm, duration of NPF = 5 h, $\sigma_{geo} = 1.7$, and GR is equal to 2 nm h^{-1} (upper panel), 4 nm h^{-1} (middle panel) or 8 nm h^{-1} (bottom panel).

considered quite typical for NPF events observed in the Beijing atmosphere.

The total number concentration of haze particles (diameter > 100 nm) originating from NPF after 48 h of subsequent particle growth follows that of the corresponding mass concentration depicted in Fig. 7, as one would expect. Noteworthy is the general number concentration level of these secondary haze particles, being typically a few hundred particles cm^{-3} when M is in the range of 10–100 μg m^{-3} and exceeding 10^3 particles cm^{-3} at high (>100 μg m^{-3}) levels of M. This means that when NPF is capable of giving a significant contribution to $PM_{2.5}$, it will also increase cloud condensation nuclei (CCN) concentrations,[49] having potentially important effects on clouds and precipitation over the region. The close connection between NPF, subsequent particle growth and notable enhancement of

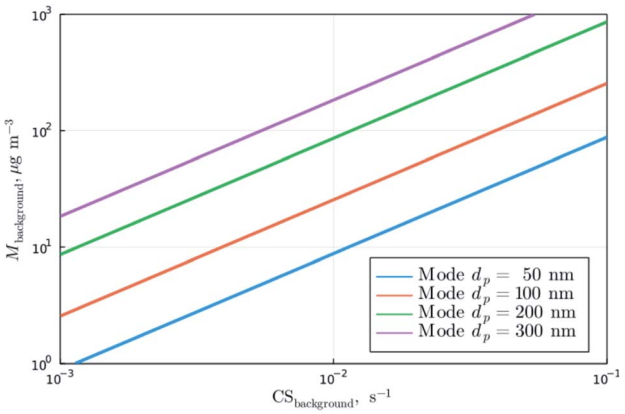

Fig. 8 Mass concentration of background aerosols as a function of their corresponding CS and mode diameter. The other model inputs are: $\sigma_{geo} = 1.7$ and $\rho = 1400$ kg m^{-3}.

CCN concentrations is consistent with earlier observation made in urban environments in China.[50]

Finally, it is interesting to look at the balance between the $PM_{2.5}$ mass concentration due to the background particle population, $M_{background}$, and that originating from NPF, M. In order to do this, we first note that submicron particulate mass is dominated by the accumulation mode and that the median diameter of this mode ranges usually between 100 and 200 nm in polluted megacities.[18,50–52] We then connect $M_{background}$ and $CS_{background}$ with each other (Fig. 8). These data show that when a background particle population starts to suppress $PM_{2.5}$ mass production originating from NPF ($CS_{background}$ > 0.01–0.04 s^{-1}), $M_{background}$ is already rather high, at least a few tens μg m^{-3} and often higher. This relation naturally holds for the opposite direction as well, having an important implication for future emission control: reducing primary particle emissions and thereby $M_{background}$ will not effective decrease the total $PM_{2.5}$ mass concentrations (M + $M_{background}$) until one simultaneous reduces emissions of precursor's cos for NPF and subsequent GTP.

4 Conclusions

We investigated the contribution of atmospheric NPF and subsequent GTP to haze, characterized by high $PM_{2.5}$ mass concentrations, using model simulations constrained with atmospheric observations in Beijing, a polluted megacity in China. We showed that the variability of the particle growth rate (GR) following NPF is relatively limited in the Beijing atmosphere, with no apparent connection with the strength of NPF or the level of background pollution. Furthermore, the GR seemed to depend only weakly on the concentration of HOMs and sulphuric acid, suggesting that more volatile vapors or multiphase chemistry are important to the overall particle growth.

Assuming conditions typically encountered in Beijing, our model simulations showed that with particle growth rates larger than about 3 nm h^{-1}, NPF and subsequent GTP often produces

more than 100 μg m^{-3} of new $PM_{2.5}$ mass. Concurrent with such $PM_{2.5}$ mass increase, significant number concentrations (up to 10^3 cm^{-3} or even more) of new haze particles (diameter > 100 nm) are formed.

Our model simulations, summarized in Fig. 7, allow us to separate three regimes in terms of NPF contributing to the production of new $PM_{2.5}$ mass: one with a low mass production (M < 10 μg m^{-3}), corresponding to either a low GR (<2–3 nm h^{-1}) of newly formed particles or a high level of background particle pollution ($CS_{background}$ > 0.01–0.04 s^{-1}), the second one with a high mass production (M > 100 μg m^{-3}), corresponding to initially clean or moderately polluted conditions ($CS_{background}$ < 0.01 s^{-1}) combined with sufficiently high new particle formation and growth rates, and the transition regime between these two (10 μg m^{-3} < M < 100 μg m^{-3}). The close connection between $CS_{background}$, $M_{background}$ and primary particle emissions (see Fig. 8), together with the strong dependency of M on $CS_{background}$ and the strength of NPF and subsequent particle growth, have an important implication for future emission control: reducing primary particle emissions and thereby $M_{background}$ will not effective decrease total $PM_{2.5}$ mass concentrations (M + $M_{background}$) unless, concomitant with primary particle emission reductions also emissions of precursor compounds for NPF and GTP will be decreased. Conceptually, these results support our hypothesized regimes for a general PM air pollution control. In this context, it could be noted that the total $PM_{2.5}$ mass concentrations have decreased over the last 10 years in Beijing,[53] while during the same period the gas-phase sulfuric acid concentration has been pretty stable.[53]

The above findings are based on observations and aerosol dynamic model simulations, but are independent of the detailed processes responsible for NPF and subsequent particle growth. However, to be able to mitigate haze, *i.e.* to reduce $PM_{2.5}$ mass or haze particle number concentrations, we need to understand the processes involved. Otherwise, it might be very difficult to control new particle formation and growth in the way that decreasing primary particle emissions will not lead to enhanced secondary $PM_{2.5}$ formation *via* NPF and GTP.

Author contributions

MK had the original idea; RC performed model calculations; CY, JJ, TP, MK planned the observations; DS, YZ, YG, CY, LD analysed the data; MK, RC, VMK analysed the results; MK and VMK wrote the first version of MS; all co-authors participated in improving and finalising the manuscript.

Conflicts of interest

There are no conflicts to declare.

Acknowledgements

We acknowledge the following projects: ACCC Flagship funded by the Academy of Finland grant number 337549, Academy professorship funded by the Academy of Finland (grant no. 302958), Academy of Finland projects no. 1325656, 316114 and 325647, "Quantifying carbon sink, CarbonSink+ and their interaction with air quality" INAR project funded by Jane and Aatos Erkko Foundation, European Research Council (ERC) project ATM-GTP Contract No. 742206, Samsung $PM_{2.5}$ SRP, the European Union's Horizon 2020 Research and Innovation Programme Marie Sklodowska-Curie grant agreement no. 895875 ("NPF-PANDA") and the Marie Skłodowska Curie ITN "CLOUD-MOTION" (764991). Technical and Scientific Staff in Beijing are acknowledged.

References

1 J. Hu, L. Huang, M. Chen, H. Liao, H. Zhang, S. Wang, Q. Zhang and Q. Ying, Premature Mortality Attributable to Particulate Matter in China: Source Contributions and Responses to Reductions, *Environ. Sci. Technol.*, 2017, **51**, 9950–9959.

2 J. Wang, B. Zhao, S. Wang, F. Yang, J. Xing, L. Morawska, A. Ding, M. Kulmala, V.-M. Kerminen, J. Kujansuu, Z. Wang, D. Ding, X. Zhang, H. Wang, M. Tian, T. Petäjä, J. Jiang and J. Hao, Particulate matter pollution over China and the effects of control policies, *Sci. Total Environ.*, 2017, **584–585**, 426–447.

3 W.-F. Ye, Z.-Y. Ma and X.-Z. Ha, Spatial-temporal patterns of PM2.5 concentrations for 338 Chinese cities, *Sci. Total Environ.*, 2018, **631–632**, 524–533.

4 J. Liu, Y. Zheng, G. Geng, C. Hong, M. Li, X. Li, F. Liu, D. Tong, R. Wu, B. Zheng, K. He and Q. Zhang, Decadal changes in anthropogenic source contribution of PM2.5 pollution and related health impacts in China, 1990–2015, *Atmos. Chem. Phys.*, 2020, **20**, 7783–7799.

5 S. Guo, M. Hu, M. L. Zamora, J. Peng, D. Shang, J. Zheng, Z. Du, Z. Wu, M. Shao, L. Zeng, M. J. Molina and R. Zhang, Elucidating severe urban haze formation in China, *Proc. Natl. Acad. Sci. U. S. A.*, 2014, **111**, 17373.

6 R. J. Huang, Y. L. Zhang, C. Bozzetti, K. F. Ho, J. J. Cao, Y. M. Han, K. R. Daellenbach, J. G. Slowik, S. M. Platt, F. Canonaco, P. Zotter, R. Wolf, S. M. Pieber, E. A. Bruns, M. Crippa, G. Ciarelli, A. Piazzalunga, M. Schwikowski, G. Abbaszade, J. Schnelle-Kreis, R. Zimmermann, Z. S. An, S. Szidat, U. Baltensperger, I. El Haddad and A. S. H. Prevot, High secondary aerosol contribution to particulate pollution during haze events in China, *Nature*, 2014, **514**, 218–222.

7 M. Kulmala, Atmospheric chemistry: China's choking cocktail, *Nature*, 2015, **526**, 497–499.

8 A. J. Ding, X. Huang, W. Nie, J. N. Sun, V. M. Kerminen, T. Petäjä, H. Su, Y. F. Cheng, X. Q. Yang, M. H. Wang, X. G. Chi, J. P. Wang, A. Virkkula, W. D. Guo, J. Yuan, S. Y. Wang, R. J. Zhang, Y. F. Wu, Y. Song, T. Zhu, S. Zilitinkevich, M. Kulmala and C. B. Fu, Enhanced haze pollution by black carbon in megacities in China, *Geophys. Res. Lett.*, 2016, **43**, 2873–2879.

9 T. Petäjä, L. Järvi, V. M. Kerminen, A. J. Ding, J. N. Sun, W. Nie, J. Kujansuu, A. Virkkula, X. Yang, C. B. Fu, S. Zilitinkevich and M. Kulmala, Enhanced air pollution

via aerosol-boundary layer feedback in China, *Sci. Rep.*, 2016, **6**, 18998.

10 Z. An, R.-J. Huang, R. Zhang, X. Tie, G. Li, J. Cao, W. Zhou, Z. Shi, Y. Han, Z. Gu and Y. Ji, Severe haze in northern China: A synergy of anthropogenic emissions and atmospheric processes, *Proc. Natl. Acad. Sci. U. S. A.*, 2019, **116**, 8657.

11 J. Zhong, X. Zhang, Y. Wang, J. Wang, X. Shen, H. Zhang, T. Wang, Z. Xie, C. Liu, H. Zhang, T. Zhao, J. Sun, S. Fan, Z. Gao, Y. Li and L. Wang, The two-way feedback mechanism between unfavorable meteorological conditions and cumulative aerosol pollution in various haze regions of China, *Atmos. Chem. Phys.*, 2019, **19**, 3287–3306.

12 X. Huang, A. Ding, Z. Wang, K. Ding, J. Gao, F. Chai and C. Fu, Amplified transboundary transport of haze by aerosol–boundary layer interaction in China, *Nat. Geosci.*, 2020, **13**, 428–434.

13 Q. Xiao, Y. Zheng, G. Geng, C. Chen, X. Huang, H. Che, X. Zhang, K. He and Q. Zhang, Separating emission and meteorological contributions to long-term PM2.5 trends over eastern China during 2000–2018, *Atmos. Chem. Phys.*, 2021, **21**, 9475–9496.

14 J. Yang and M. Shao, Impacts of Extreme Air Pollution Meteorology on Air Quality in China, *J. Geophys. Res.: Atmos.*, 2021, **126**, e2020JD033210.

15 M. Kulmala, L. Dada, K. R. Daellenbach, C. Yan, D. Stolzenburg, J. Kontkanen, E. Ezhova, S. Hakala, S. Tuovinen, T. V. Kokkonen, M. Kurppa, R. Cai, Y. Zhou, R. Yin, R. Baalbaki, T. Chan, B. Chu, C. Deng, Y. Fu, M. Ge, H. He, L. Heikkinen, H. Junninen, Y. Liu, Y. Lu, W. Nie, A. Rusanen, V. Vakkari, Y. Wang, G. Yang, L. Yao, J. Zheng, J. Kujansuu, J. Kangasluoma, T. Petäjä, P. Paasonen, L. Järvi, D. Worsnop, A. Ding, Y. Liu, L. Wang, J. Jiang, F. Bianchi and V.-M. Kerminen, Is reducing new particle formation a plausible solution to mitigate particulate air pollution in Beijing and other Chinese megacities?, *Faraday Discuss.*, 2021, **226**, 334–347.

16 T. Rönkkö, H. Kuuluvainen, P. Karjalainen, J. Keskinen, R. Hillamo, J. V. Niemi, L. Pirjola, H. J. Timonen, S. Saarikoski, E. Saukko, A. Järvinen, H. Silvennoinen, A. Rostedt, M. Olin, J. Yli-Ojanperä, P. Nousiainen, A. Kousa and M. Dal Maso, Traffic is a major source of atmospheric nanocluster aerosol, *Proc. Natl. Acad. Sci. U. S. A.*, 2017, **114**, 7549.

17 J. Kontkanen, C. Deng, Y. Fu, L. Dada, Y. Zhou, J. Cai, K. R. Daellenbach, S. Hakala, T. V. Kokkonen, Z. Lin, Y. Liu, Y. Wang, C. Yan, T. Petäjä, J. Jiang, M. Kulmala and P. Paasonen, Size-resolved particle number emissions in Beijing determined from measured particle size distributions, *Atmos. Chem. Phys.*, 2020, **20**, 11329–11348.

18 Y. Zhou, L. Dada, Y. Liu, Y. Fu, J. Kangasluoma, T. Chan, C. Yan, B. Chu, K. R. Daellenbach, F. Bianchi, T. V. Kokkonen, Y. Liu, J. Kujansuu, V. M. Kerminen, T. Petäjä, L. Wang, J. Jiang and M. Kulmala, Variation of size-segregated particle number concentrations in wintertime Beijing, *Atmos. Chem. Phys.*, 2020, **20**, 1201–1216.

19 M. Kulmala, V. M. Kerminen, T. Petäjä, A. J. Ding and L. Wang, Atmospheric gas-to-particle conversion: why NPF events are observed in megacities?, *Faraday Discuss.*, 2017, **200**, 271–288.

20 Y. Liu, C. Yan, Z. Feng, F. Zheng, X. Fan, Y. Zhang, C. Li, Y. Zhou, Z. Lin, Y. Guo, Y. Zhang, L. Ma, W. Zhou, Z. Liu, L. Dada, K. Dällenbach, J. Kontkanen, R. Cai, T. Chan, B. Chu, W. Du, L. Yao, Y. Wang, J. Cai, J. Kangasluoma, T. Kokkonen, J. Kujansuu, A. Rusanen, C. Deng, Y. Fu, R. Yin, X. Li, Y. Lu, Y. Liu, C. Lian, D. Yang, W. Wang, M. Ge, Y. Wang, D. R. Worsnop, H. Junninen, H. He, V.-M. Kerminen, J. Zheng, L. Wang, J. Jiang, T. Petäjä, F. Bianchi and M. Kulmala, Continuous and comprehensive atmospheric observations in Beijing: a station to understand the complex urban atmospheric environment, *Big Earth Data*, 2020, **4**, 295–321.

21 S. Mirme and A. Mirme, The mathematical principles and design of the NAIS – a spectrometer for the measurement of cluster ion and nanometer aerosol size distributions, *Atmos. Meas. Tech.*, 2013, **6**, 1061–1071.

22 R. Cai, D.-R. Chen, J. Hao and J. Jiang, A miniature cylindrical differential mobility analyzer for sub-3 nm particle sizing, *J. Aerosol Sci.*, 2017, **106**, 111–119.

23 Y. Fu, M. Xue, R. Cai, J. Kangasluoma and J. Jiang, Theoretical and experimental analysis of the core sampling method: Reducing diffusional losses in aerosol sampling line, *Aerosol Sci. Technol.*, 2019, **53**, 793–801.

24 J. Jiang, M. Chen, C. Kuang, M. Attoui and P. H. McMurry, Electrical Mobility Spectrometer Using a Diethylene Glycol Condensation Particle Counter for Measurement of Aerosol Size Distributions Down to 1 nm, *Aerosol Sci. Technol.*, 2011, **45**, 510–521.

25 C. Yan, R. Yin, Y. Lu, L. Dada, D. Yang, Y. Fu, J. Kontkanen, C. Deng, O. Garmash, J. Ruan, R. Baalbaki, M. Schervish, R. Cai, M. Bloss, T. Chan, T. Chen, Q. Chen, X. Chen, Y. Chen, B. Chu, K. Dällenbach, B. Foreback, X. He, L. Heikkinen, T. Jokinen, H. Junninen, J. Kangasluoma, T. Kokkonen, M. Kurppa, K. Lehtipalo, H. Li, H. Li, X. Li, Y. Liu, Q. Ma, P. Paasonen, P. Rantala, R. E. Pileci, A. Rusanen, N. Sarnela, P. Simonen, S. Wang, W. Wang, Y. Wang, M. Xue, G. Yang, L. Yao, Y. Zhou, J. Kujansuu, T. Petäjä, W. Nie, Y. Ma, M. Ge, H. He, N. M. Donahue, D. R. Worsnop, K. Veli-Matti, L. Wang, Y. Liu, J. Zheng, M. Kulmala, J. Jiang and F. Bianchi, The Synergistic Role of Sulfuric Acid, Bases, and Oxidized Organics Governing New-Particle Formation in Beijing, *Geophys. Res. Lett.*, 2021, **48**, e2020GL091944.

26 C. Deng, Y. Fu, L. Dada, C. Yan, R. Cai, D. Yang, Y. Zhou, R. Yin, Y. Lu, X. Li, X. Qiao, X. Fan, W. Nie, J. Kontkanen, J. Kangasluoma, B. Chu, A. Ding, V. Kerminen, P. Paasonen, R. D. Worsnop, F. Bianchi, Y. Liu, J. Zheng, L. Wang, M. Kulmala and J. Jiang, Seasonal characteristics of new particle formation and growth in urban Beijing, *Environ. Sci. Technol.*, 2020, **54**, 8547–8557.

27 L. Dada, K. Lehtipalo, J. Kontkanen, T. Nieminen, R. Baalbaki, L. Ahonen, J. Duplissy, C. Yan, B. Chu, T. Petäjä, K. Lehtinen, V.-M. Kerminen, M. Kulmala and

J. Kangasluoma, Formation and growth of sub-3-nm aerosol particles in experimental chambers, *Nat. Protoc.*, 2020, **15**, 1013–1040.

28 K. Lehtipalo, J. Leppa, J. Kontkanen, J. Kangasluoma, A. Franchin, D. Wimmer, S. Schobesberger, H. Junninen, T. Petaja, M. Sipila, J. Mikkila, J. Vanhanen, D. R. Worsnop and M. Kulmala, Methods for determining particle size distribution and growth rates between 1 and 3 nm using the Particle Size Magnifier, *Boreal Environ. Res.*, 2014, **19**, SS215+.

29 M. Kulmala, T. Petäjä, T. Nieminen, M. Sipilä, H. E. Manninen, K. Lehtipalo, M. Dal Maso, P. P. Aalto, H. Junninen, P. Paasonen, I. Riipinen, K. E. J. Lehtinen, A. Laaksonen and V.-M. Kerminen, Measurement of the nucleation of atmospheric aerosol particles, *Nat. Protoc.*, 2012, **7**, 1651–1667.

30 V.-M. Kerminen and M. Kulmala, Analytical formulae connecting the "real" and the "apparent" nucleation rate and the nuclei number concentration for atmospheric nucleation events, *J. Aerosol Sci.*, 2002, **33**, 609–622.

31 K. E. J. Lehtinen, M. Dal Maso, M. Kulmala and V.-M. Kerminen, Estimating nucleation rates from apparent particle formation rates and vice versa: Revised formulation of the Kerminen–Kulmala equation, *J. Aerosol Sci.*, 2007, **38**, 988–994.

32 T. Anttila, V.-M. Kerminen and K. E. J. Lehtinen, Parameterizing the formation rate of new particles: The effect of nuclei self-coagulation, *J. Aerosol Sci.*, 2010, **41**, 621–636.

33 T. Hatch and S. P. Choate, Statistical description of the size properties of non uniform particulate substances, *J. Franklin Inst.*, 1929, **207**, 369–387.

34 V.-M. Kerminen, K. E. J. Lehtinen, T. Anttila and M. Kulmala, Dynamics of atmospheric nucleation mode particles: a timescale analysis, *Tellus B: Chemical and Physical Meteorology*, 2004, **56**, 135–146.

35 D. L. Yue, M. Hu, R. Y. Zhang, Z. B. Wang, J. Zheng, Z. J. Wu, A. Wiedensohler, L. Y. He, X. F. Huang and T. Zhu, The roles of sulfuric acid in new particle formation and growth in the mega-city of Beijing, *Atmos. Chem. Phys.*, 2010, **10**, 4953–4960.

36 C. J. Williamson, A. Kupc, D. Axisa, K. R. Bilsback, T. Bui, P. Campuzano-Jost, M. Dollner, K. D. Froyd, A. L. Hodshire, J. L. Jimenez, J. K. Kodros, G. Luo, D. M. Murphy, B. A. Nault, E. A. Ray, B. Weinzierl, J. C. Wilson, F. Yu, P. Yu, J. R. Pierce and C. A. Brock, A large source of cloud condensation nuclei from new particle formation in the tropics, *Nature*, 2019, **574**, 399–403.

37 L. Wang, A. F. Khalizov, J. Zheng, W. Xu, Y. Ma, V. Lal and R. Zhang, Atmospheric nanoparticles formed from heterogeneous reactions of organics, *Nat. Geosci.*, 2010, **3**, 238–242.

38 I. Riipinen, T. Yli-Juuti, J. R. Pierce, T. Petäjä, D. R. Worsnop, M. Kulmala and N. M. Donahue, The contribution of organics to atmospheric nanoparticle growth, *Nat. Geosci.*, 2012, **5**, 453–458.

39 M. Riva, J. Sun, V. F. McNeill, C. Ragon, S. Perrier, Y. Rudich, S. A. Nizkorodov, J. Chen, F. Caupin, T. Hoffmann and C. George, High Pressure Inside Nanometer-Sized Particles Influences the Rate and Products of Chemical Reactions, *Environ. Sci. Technol.*, 2021, **55**, 7786–7793.

40 E. Herrmann, A. J. Ding, V. M. Kerminen, T. Petäjä, X. Q. Yang, J. N. Sun, X. M. Qi, H. Manninen, J. Hakala, T. Nieminen, P. P. Aalto, M. Kulmala and C. B. Fu, Aerosols and nucleation in eastern China: first insights from the new SORPES-NJU station, *Atmos. Chem. Phys.*, 2014, **14**, 2169–2183.

41 L. Yao, O. Garmash, F. Bianchi, J. Zheng, C. Yan, J. Kontkanen, H. Junninen, S. B. Mazon, M. Ehn, P. Paasonen, M. Sipila, M. Y. Wang, X. K. Wang, S. Xiao, H. F. Chen, Y. Q. Lu, B. W. Zhang, D. F. Wang, Q. Y. Fu, F. H. Geng, L. Li, H. L. Wang, L. P. Qiao, X. Yang, J. M. Chen, V. M. Kerminen, T. Petaja, D. R. Worsnop, M. Kulmala and L. Wang, Atmospheric new particle formation from sulfuric acid and amines in a Chinese megacity, *Science*, 2018, **361**, 278–281.

42 B. Chu, V. M. Kerminen, F. Bianchi, C. Yan, T. Petäjä and M. Kulmala, Atmospheric new particle formation in China, *Atmos. Chem. Phys.*, 2019, **19**, 115–138.

43 C. Deng, Y. Fu, L. Dada, C. Yan, R. Cai, D. Yang, Y. Zhou, R. Yin, Y. Lu, X. Li, X. Qiao, X. Fan, W. Nie, J. Kontkanen, J. Kangasluoma, B. Chu, A. Ding, V.-M. Kerminen, P. Paasonen, D. R. Worsnop, F. Bianchi, Y. Liu, J. Zheng, L. Wang, M. Kulmala and J. Jiang, Seasonal Characteristics of New Particle Formation and Growth in Urban Beijing, *Environ. Sci. Technol.*, 2020, **54**, 8547–8557.

44 X. Shen, J. Sun, F. Yu, Y. Wang, J. Zhong, Y. Zhang, X. Hu, C. Xia, S. Zhang and X. Zhang, Enhancement of nanoparticle formation and growth during the COVID-19 lockdown period in urban Beijing, *Atmos. Chem. Phys.*, 2021, **21**, 7039–7052.

45 S. Yang, Z. Liu, P. S. Clusius, Y. Liu, J. Zou, Y. Yang, S. Zhao, G. Zhang, Z. Xu, Z. Ma, Y. Yang, J. Sun, Y. Pan, D. Ji, B. Hu, C. Yan, M. Boy, M. Kulmala and Y. Wang, Chemistry of new particle formation and growth events during wintertime in suburban area of Beijing: Insights from highly polluted atmosphere, *Atmos. Res.*, 2021, **255**, 105553.

46 J. R. Pierce and P. J. Adams, Efficiency of cloud condensation nuclei formation from ultrafine particles, *Atmos. Chem. Phys.*, 2007, **7**, 1367–1379.

47 Z. Wu, M. Hu, S. Liu, B. Wehner, S. Bauer, A. Ma ßling, A. Wiedensohler, T. Petäjä, M. Dal Maso and M. Kulmala, New particle formation in Beijing, China: Statistical analysis of a 1-year data set, *J. Geophys. Res.: Atmos.*, 2007, **112**, D09209.

48 D. Yue, M. Hu, Z. Wu, Z. Wang, S. Guo, B. Wehner, A. Nowak, P. Achtert, A. Wiedensohler, J. Jung, Y. J. Kim and S. Liu, Characteristics of aerosol size distributions and new particle formation in the summer in Beijing, *J. Geophys. Res.: Atmos.*, 2009, **114**, D00G12.

49 Z. B. Wang, M. Hu, J. Y. Sun, Z. J. Wu, D. L. Yue, X. J. Shen, Y. M. Zhang, X. Y. Pei, Y. F. Cheng and A. Wiedensohler, Characteristics of regional new particle formation in urban

and regional background environments in the North China Plain, *Atmos. Chem. Phys.*, 2013, **13**, 12495–12506.

50 J. F. Peng, M. Hu, Z. B. Wang, X. F. Huang, P. Kumar, Z. J. Wu, S. Guo, D. L. Yue, D. J. Shang, Z. Zheng and L. Y. He, Submicron aerosols at thirteen diversified sites in China: size distribution, new particle formation and corresponding contribution to cloud condensation nuclei production, *Atmos. Chem. Phys.*, 2014, **14**, 10249–10265.

51 X. M. Qi, A. J. Ding, W. Nie, T. Petäjä, V. M. Kerminen, E. Herrmann, Y. N. Xie, L. F. Zheng, H. Manninen, P. Aalto, J. N. Sun, Z. N. Xu, X. G. Chi, X. Huang, M. Boy, A. Virkkula, X. Q. Yang, C. B. Fu and M. Kulmala, Aerosol size distribution and new particle formation in the western Yangtze River Delta of China: 2 years of measurements at the SORPES station, *Atmos. Chem. Phys.*, 2015, **15**, 12445–12464.

52 S. Gani, S. Bhandari, K. Patel, S. Seraj, P. Soni, Z. Arub, G. Habib, L. Hildebrandt Ruiz and J. S. Apte, Particle number concentrations and size distribution in a polluted megacity: the Delhi Aerosol Supersite study, *Atmos. Chem. Phys.*, 2020, **20**, 8533–8549.

53 X. Li, B. Zhao, W. Zhou, H. Shi, R. Yin, R. Cai, D. Yang, K. Dällebach, C. Deng, Y. Fu, X. Qiao, L. Wang, Y. Liu, C. Yan, M. Kulmala, J. Zheng, J. Hao, S. Wang and J. Jiang, Responses of gaseous sulfuric acid and particulate sulfate to reduced SO_2 concentration: A perspective from long-term measurements in Beijing, *Sci. Total Environ.*, 2020, **721**, 137700.